Electronic Supplementary Material (ESI) for Physical Chemistry Chemical Physics.

Supporting Information: Theoretical Predictions of Novel Potassium Chloride Phases Under Pressure

Andrew Shamp, Patrick Saitta, Eva Zurek

Contents

1 Structure Search - Technical Details

XTALOPT uses a continuous mode of operation that procreates a new offspring immediately after an individual finishes optimizing, instead of waiting for an entire generation to complete. The parents are taken from a population-based pool rather than a generation-based one and a "generation" in XTALOPT denotes the number of individuals that separate a structure from the initial set. Table 1 provides the number of formula units we employed in each structure search and the size of the total population in a given run. We generally stopped each run after the lowest-enthalpy structure was recovered at least three times and remained unchanged over at least 100 structures. All runs were conducted using a six-step structural optimization scheme; this scheme refers to the series of electronic structure calculations used to optimize each geometry generated by XTALOPT. That is, the (n + 1)th optimization step employed for each geometry uses the optimized structure from the nth step as a starting geometry. The 1st and 2nd step allowed only the ions to relax, but the remaining 4 steps allowed both the ions and lattice parameters to relax during the optimization. The precision of the calculation was increased in each optimization step.

Stoichiometry	Number of Formula Units	Pressure (GPa)	Population	Potential Type
KCl	2	200	20	Normal
		300	178	Normal
	3	200	80	Normal
		300	197	Hard
		600	438	Hard
	4	2	154	Normal
		25	488	Hard
		100	210	Hard
		150	151	Hard
		250	419	Hard
		300	218	Normal
		300	158	Hard
		600	627	Hard

Table S1: Number of formula units, pressure, size of the population, and PAW type employed in the evolutionary structure searches.

2 Structural Parameters and Atomic Positions

Structure	Pressure (GPa)	a (Å)	b (Å)	c (Å)	α, β, γ (Θ)	Atom	Wyckoff Position
Fm$\bar{3}$*m*	1	6.28	6.28	6.28	90.00	Cl	4b: (0.50000, 0.50000, 0.50000)
						K	4a: (0.00000, 0.00000, 0.00000)
Pm$\bar{3}$*m*	5	3.62	3.62	3.62	90.00	Cl	1a: (0.00000, 0.00000, 0.00000)
						K	1b: (0.50000, 0.50000, 0.50000)
I4$_1$*/amd*	200	3.40	3.40	7.04	90.00	Cl	4b: (0.00000, 0.25000, 0.37500)
						K	4a: (0.00000, 0.75000, 0.12500)
Pnma	350	3.96	3.76	4.54	90.00	Cl	4c: (0.58511, 0.25000, 0.37518)
						K	4c: (0.08709, 0.25000, 0.62425)

Table S2: Calculated structural parameters of the most stable phases of potassium chloride at various pressures.

3 Structure Nearest Neighbors Comparisons

The T1 structure was found to be less stable than both the known KCl phases and the ones predicted in this paper. This can be explained by considering the nearest neighbor contacts within the structure and the Coulombic repulsion or attraction that would result from these contacts. Starting with the B1 structure each potassium atom has 6 chlorines as its nearest neighbors (2.421 Å at 100 GPa) in an octahedral arrangement. Moving onto the B2 structure each potassium has 8 chlorine nearest neighbors (2.547 Å at 100 GPa) in a cubic arrangement. The T1 structure, on the other hand, has two symmetry inequivalent potassiums and one chlorine. The first potassium is surrounded by exactly the same number of chlorines as in the B2 structure and in the same arrangement (2.642 Å at 100 GPa). The second potassium, however, has 6 nearest neighbors, 4 of which are chlorines (2.311 Å) but the other 2 are potassiums (2.561 Å). Each chlorine has 8 nearest neighbors: 2 potassium (2.311 Å), 2 chlorine (2.561 Å), and 4 potassium (2.642 Å). The potassiums are positively charged and the chlorines are negatively charged. The close proximity of ions of the same charge in the T1 structure results in a large Coulombic repulsion that causes it to have a higher enthalpy as compared to the other structures. In comparison, within the higher pressure $I4_1/amd$ phase each potassium has 8 chlorine nearest neighbors at 2.354 Å, 4 more at

2.384 Å, and 4 potassiums at 2.384 Å at 250 GPa.

4 $Fm\bar{3}m$ Electronic and Phonon Density of States and Electronic Band Structure

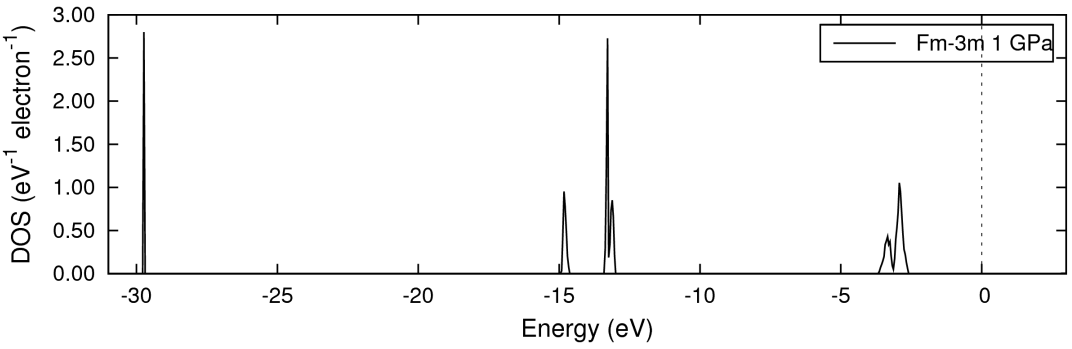

Figure S1: Electronic density of states for the $Fm\bar{3}m$ KCl phase at 1 GPa. The Fermi level has been set to zero.

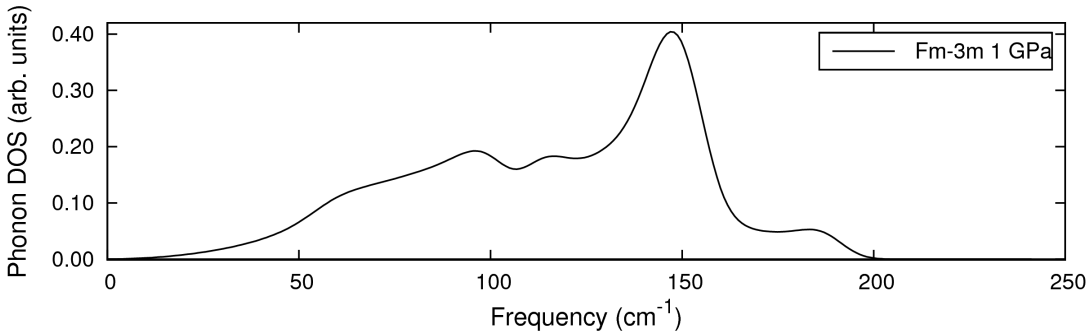

Figure S2: Calculated phonon density of states for $Fm\bar{3}m$ at 1 GPa.

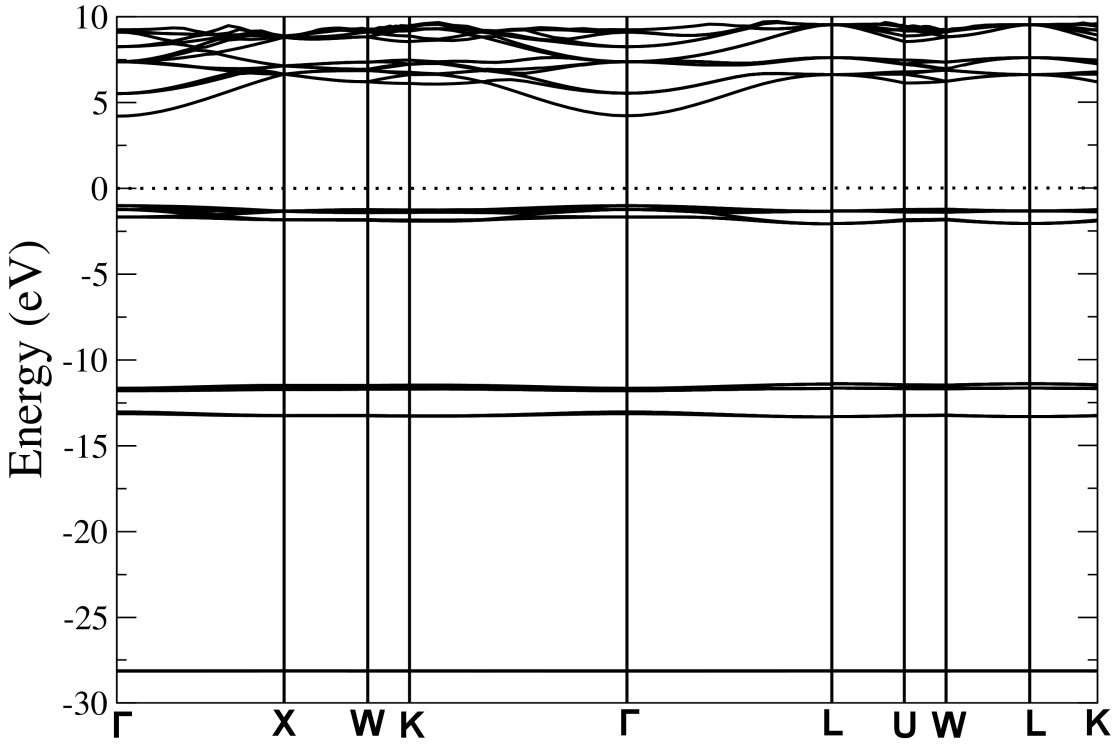

Figure S3: Electronic band structures of $Fm\bar{3}m$ at 1 GPa.

5 *Pm*$\bar{3}$*m* Electronic and Phonon Density of States and Electronic Band Structure

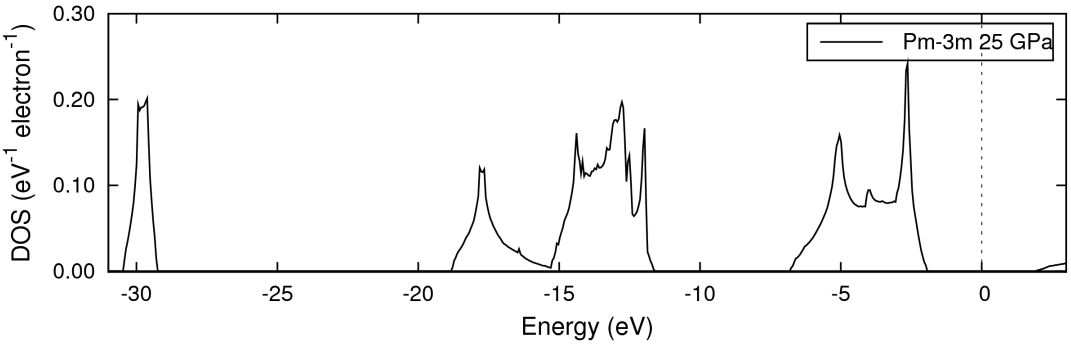

Figure S4: Electronic density of states for the *Pm*$\bar{3}$*m* KCl phase at 25 GPa. The Fermi level has been set to zero.

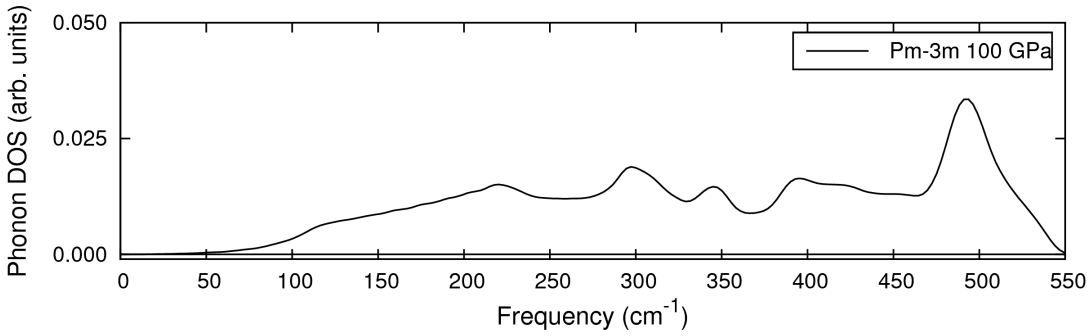

Figure S5: Calculated phonon density of states for $Pm\bar{3}m$ at 100 GPa.

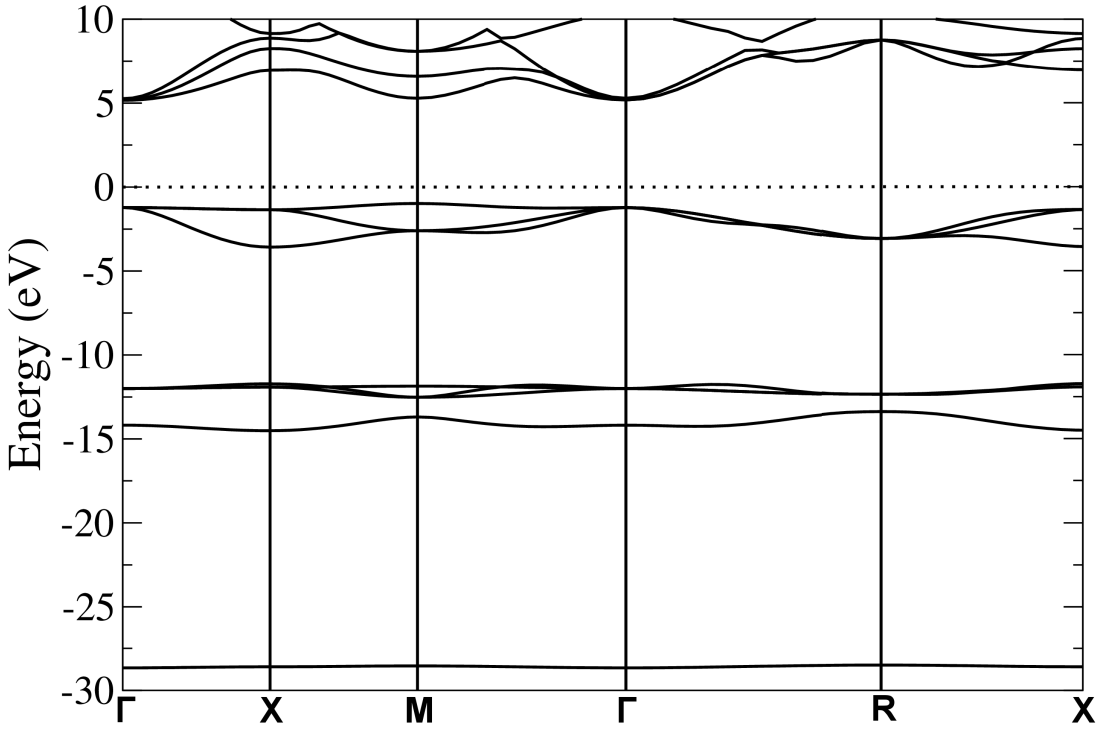

Figure S6: Electronic band structures of $Pm\bar{3}m$ at 10 GPa.

6 Electronic and Phonon Density of States, Band Structures, and Powder Diffraction Patterns of *I4*$_1$*/amd*-KCl

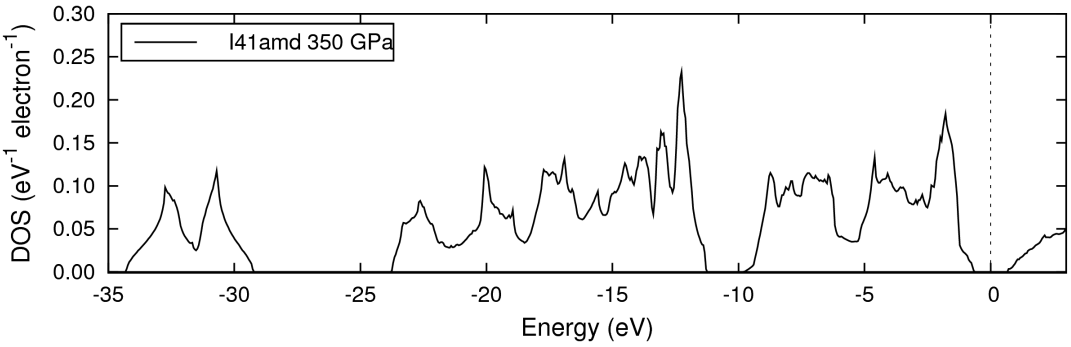

Figure S7: Electronic density of states for the *I4*$_1$*/amd* KCl phase at 350 GPa. The Fermi level has been set to zero.

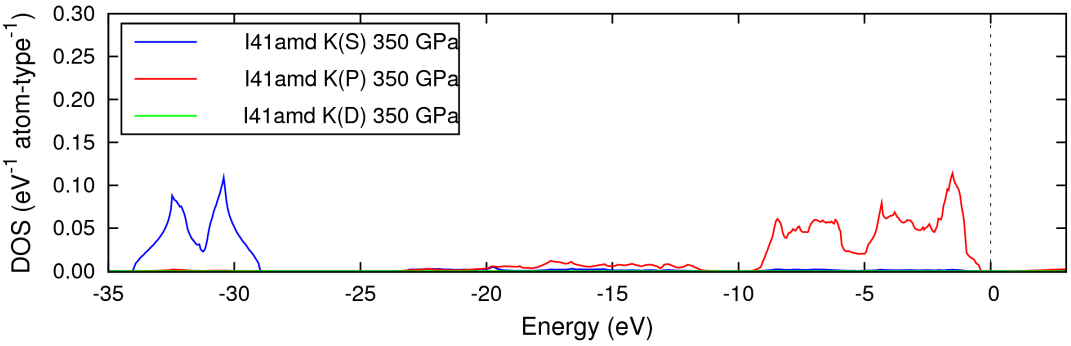

Figure S8: Electronic density of states for the *I4*$_1$*/amd* KCl phase at 350 GPa projected onto K *spd* angular momenta. The Fermi level has been set to zero.

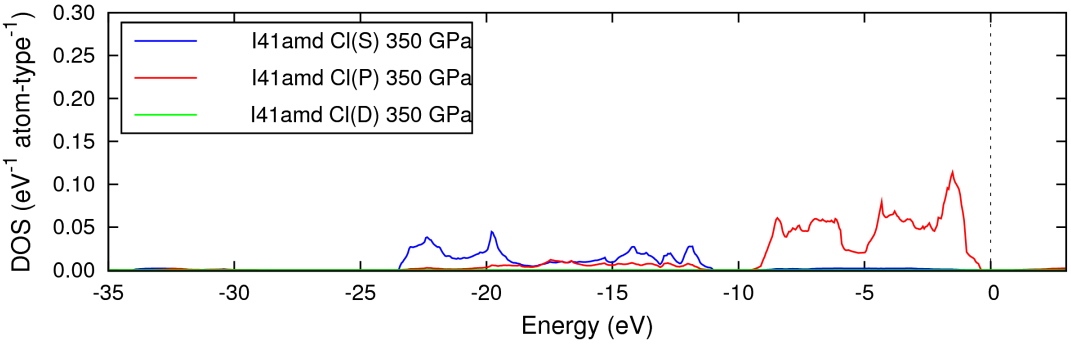

Figure S9: Electronic density of states for the $I4_1/amd$ KCl phase at 350 GPa projected onto Cl spd angular momenta. The Fermi level has been set to zero.

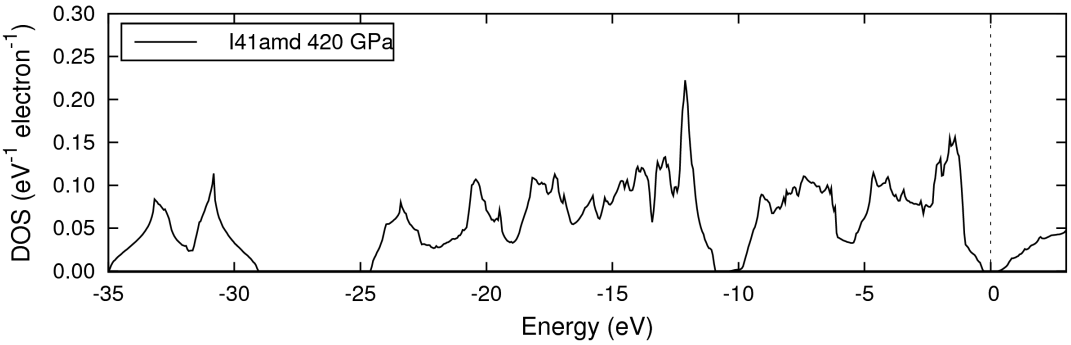

Figure S10: Electronic density of states for the $I4_1/amd$ KCl phase at 420 GPa. The Fermi level has been set to zero.

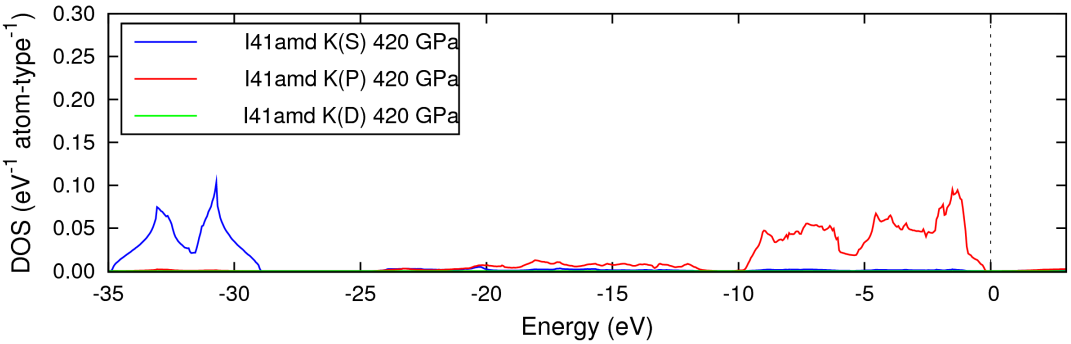

Figure S11: Electronic density of states for the $I4_1/amd$ KCl phase at 420 GPa projected onto K spd angular momenta.. The Fermi level has been set to zero.

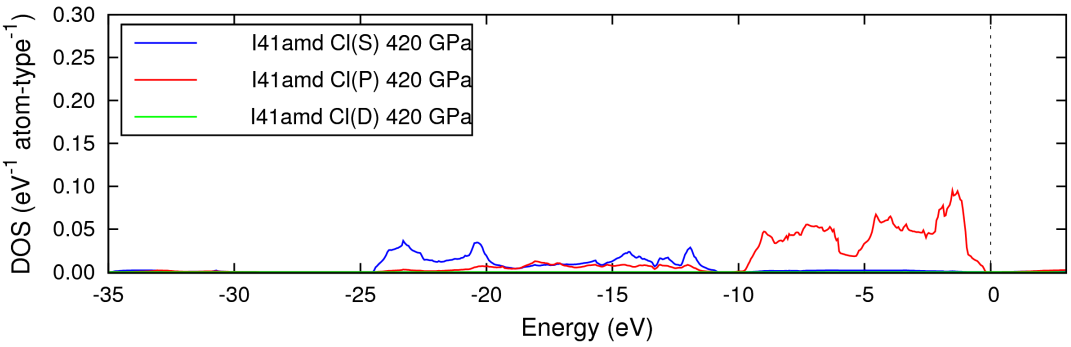

Figure S12: Electronic density of states for the $I4_1/amd$ KCl phase at 420 GPa projected onto Cl spd angular momenta.

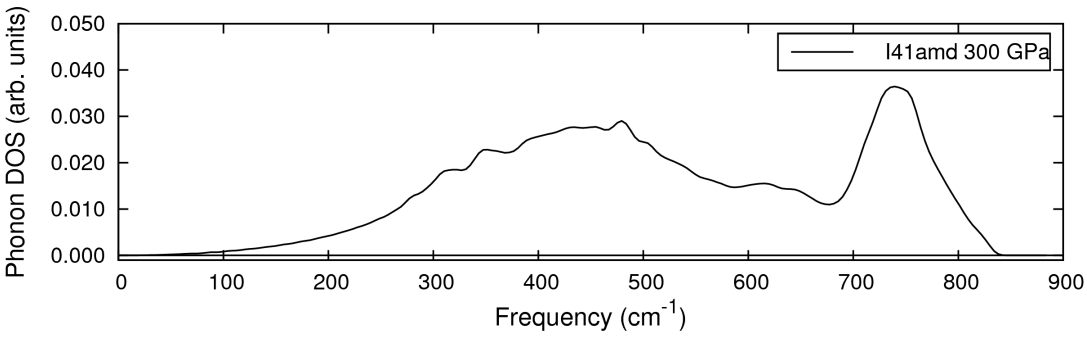

Figure S13: Calculated phonon density of states for $I4_1/amd$ at 300 GPa.

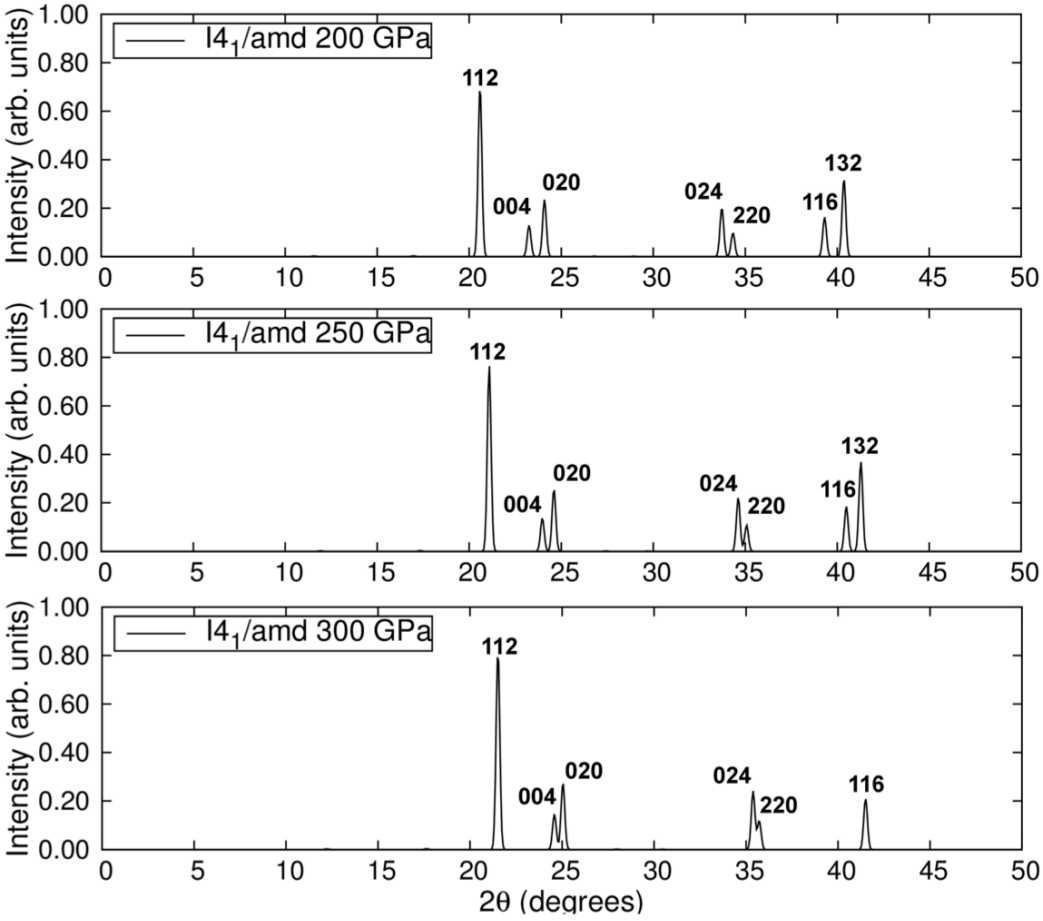

Figure S14: Simulated X-ray powder diffraction pattern for $I4_1/amd$-KCl at 200, 250, and 300 GPa (simulated using an Mo X-ray source, $\lambda = 0.7093$ Å, and a Gaussian broadening with σ=0.1 θ).

7 Electronic and Phonon Density of States, Band Structures, and Powder Diffraction Patterns of $Pnma$-KCl

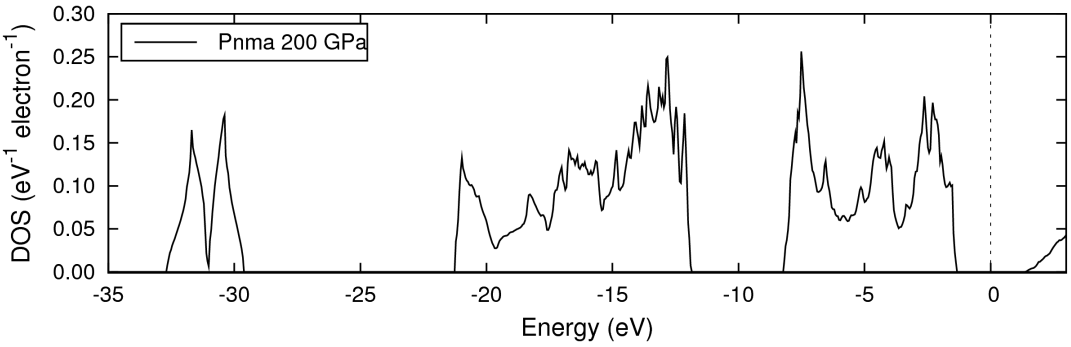

Figure S15: Electronic density of states for the *Pnma* KCl phase at 200 GPa. The Fermi level has been set to zero.

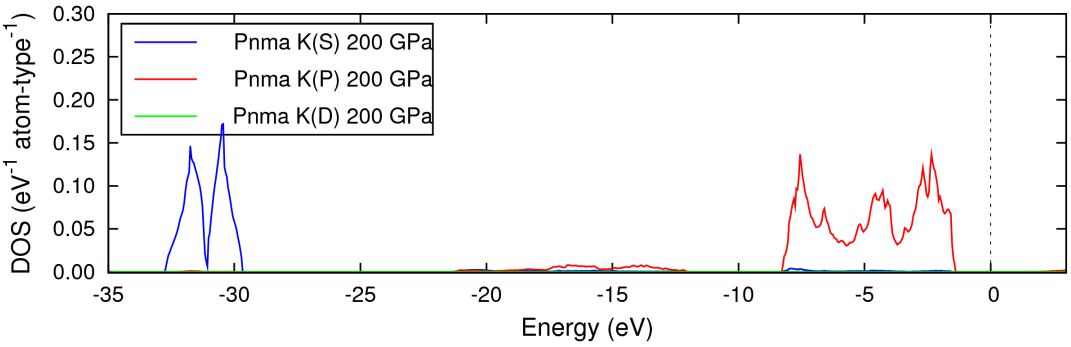

Figure S16: Electronic density of states for the *Pnma* KCl phase at 200 GPa projected onto K spd angular momenta.. The Fermi level has been set to zero.

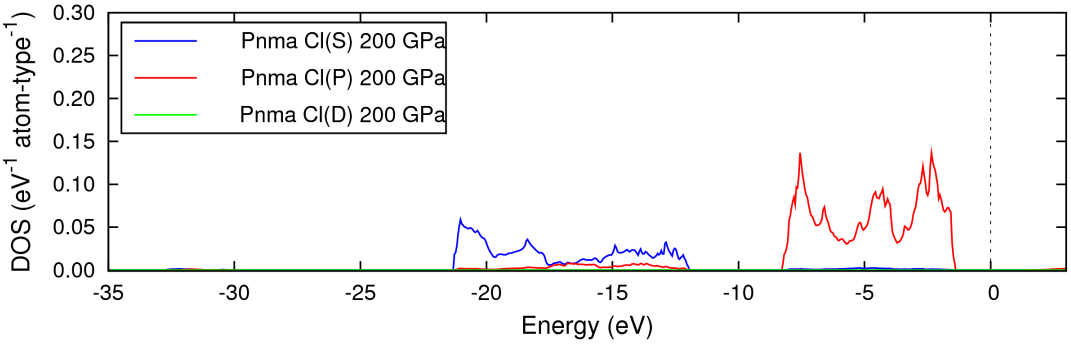

Figure S17: Electronic density of states for the *Pnma* KCl phase at 200 GPa projected onto Cl spd angular momenta.. The Fermi level has been set to zero.

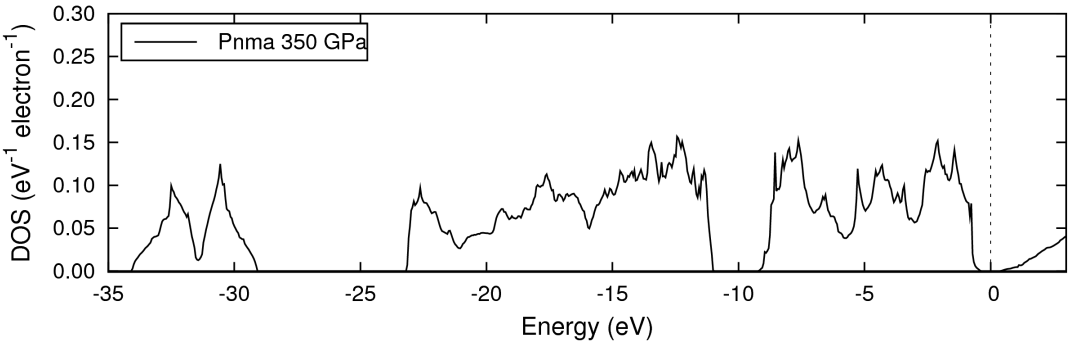

Figure S18: Electronic density of states for the *Pnma* KCl phase at 350 GPa. The Fermi level has been set to zero.

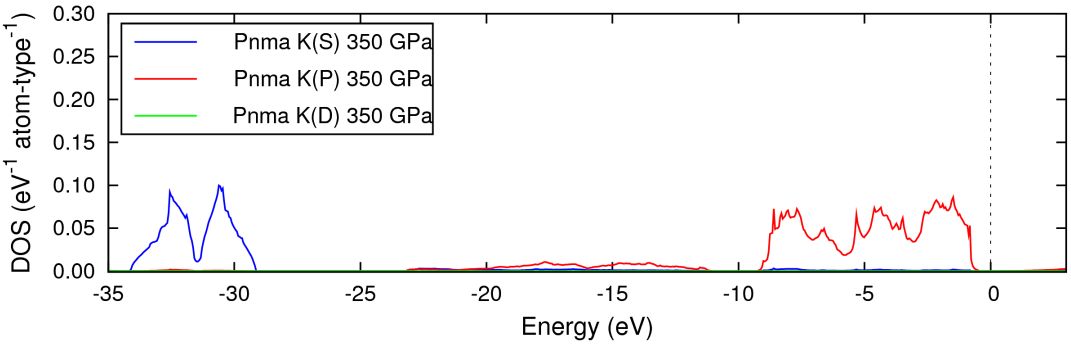

Figure S19: Electronic density of states for the *Pnma* KCl phase at 350 GPa projected onto K spd angular momenta.. The Fermi level has been set to zero.

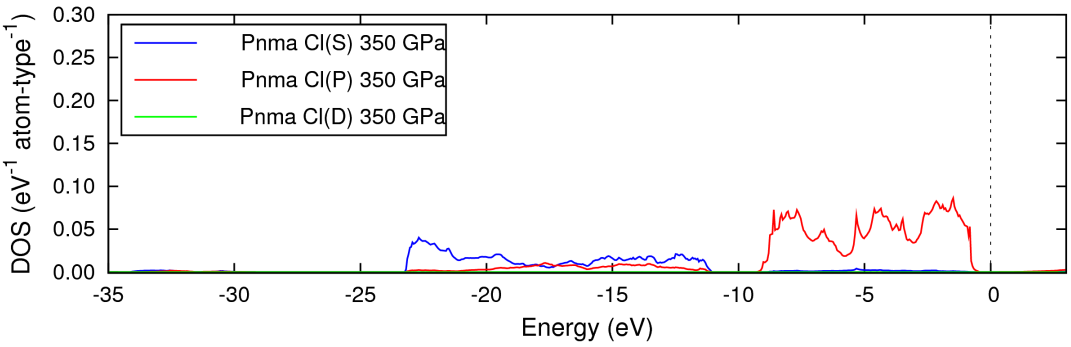

Figure S20: Electronic density of states for the *Pnma* KCl phase at 350 GPa projected onto K *spd* angular momenta.. The Fermi level has been set to zero.

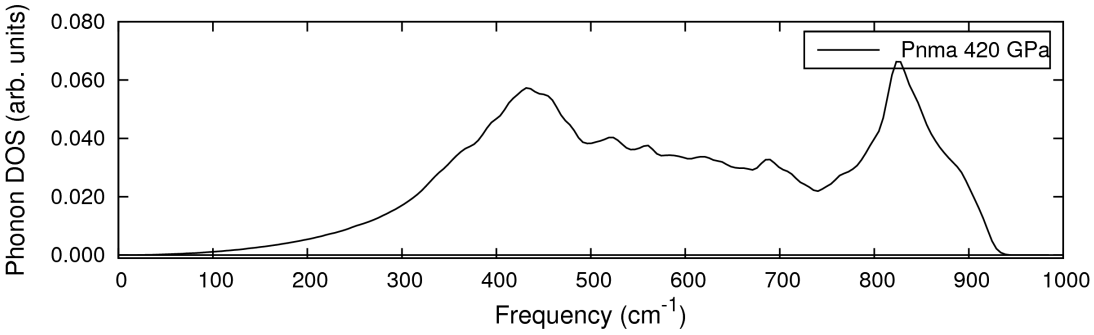

Figure S21: Calculated phonon density of states for *Pnma* at 420 GPa.

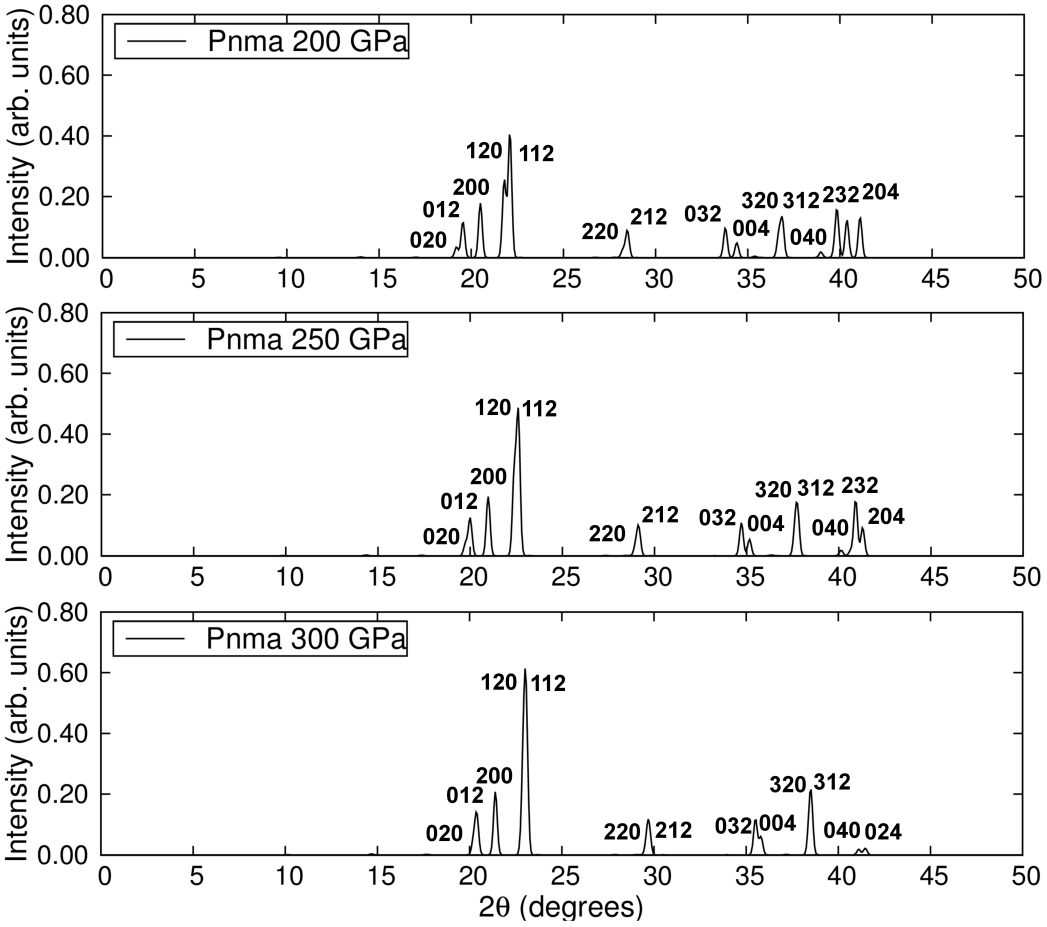

Figure S22: Simulated X-ray powder diffraction pattern for $Pnma$-KCl at 200, 250, and 300 GPa (simulated using an Mo X-ray source, $\lambda = 0.7093$ Å, and a Gaussian broadening with σ=0.1 θ).